PROCEEDINGS OF THE ROYAL SOCIETY B BIOLOGICAL SCIENCES

Plankton reach new heights in effort to avoid predators

Brad J. Gemmell, Houshuo Jiang, J. Rudi Strickler and Edward J. Buskey

Proc. R. Soc. B 2012 **279**, 2786-2792 first published online 21 March 2012
doi: 10.1098/rspb.2012.0163

PROCEEDINGS OF THE ROYAL SOCIETY B

Proc. R. Soc. B (2012) **279**, 2786–2792
doi:10.1098/rspb.2012.0163
Published online 21 March 2012

Plankton reach new heights in effort to avoid predators

Brad J. Gemmell[1,*], Houshuo Jiang[2], J. Rudi Strickler[3] and Edward J. Buskey[1]

[1]*Marine Science Institute, University of Texas at Austin, 750 Channel View Dr, Port Aransas, TX 78373, USA*
[2]*Woods Hole Oceanographic Institution, Mailstop 11, Woods Hole, MA 02543, USA*
[3]*WATER Institute, University of Wisconsin Milwaukee, 600 East Greenfield Avenue, Milwaukee, WI 53204, USA*

The marine environment associated with the air–water interface (neuston) provides an important food source to pelagic organisms where subsurface prey is limited. However, studies on predator–prey interactions within this environment are lacking. Copepods are known to produce strong escape jumps in response to predators, but must contend with a low-Reynolds-number environment where viscous forces limit escape distance. All previous work on copepod interaction with predators has focused on a liquid environment. Here, we describe a novel anti-predator behaviour in two neustonic copepod species, where individuals frequently exit the water surface and travel many times their own body length through air to avoid predators. Using both field recordings with natural predators and high-speed laboratory recordings, we obtain detailed kinematics of this behaviour, and estimate energetic cost associated with this behaviour. We demonstrate that despite losing up to 88 per cent of their initial kinetic energy, copepods that break the water surface travel significantly further than those escaping underwater and successfully exit the perceptive field of the predator. This behaviour provides an effective defence mechanism against subsurface-feeding visual predators and the results provide insight into trophic interactions within the neustonic environment.

Keywords: predation; neuston; aerial escape; copepod; fish; perceptive field

1. INTRODUCTION

Copepods are among the most abundant metazoans on the planet [1,2], and are known to be important prey for fish [3–6] and other marine organisms [7,8]. The copepod's role in marine food webs makes their behavioural adaptations to predation important to understand. The neustonic environment consists of the upper few millimetres of water associated with the air–water interface. This environment is often characterized by elevated biomass and numbers of organisms relative to the water beneath [9], and it provides food to higher tropic levels such as fish [10]. Pontellid copepods are a ubiquitous group often found in neustonic environments, and adults are known to reside during daylight hours in the brightly lit surface water of coastal oceans [11].

Many planktonic organisms residing in the photic zone have nearly transparent tissues, which are assumed to reduce conspicuousness to visual predators [12]. However, species that live in close proximity to the water surface (neuston) are often highly pigmented, including copepods [13]. Pigmentation in copepods has been demonstrated to reduce the effects of damaging UV radiation [14,15] and may play a similar role in pontellids. These copepods are also large in comparison with many other copepod taxa [16]. This large size, combined with pigmentation, makes these copepods more visually conspicuous, and thus should be preferred by visual fish predators [17,18].

* Author for correspondence (bgemmell@mbl.edu).

Electronic supplementary material is available at http://dx.doi.org/10.1098/rspb.2012.0163 or via http://rspb.royalsocietypublishing.org.

One of the mechanisms by which copepods are known to avoid fish predators is through the use of powerful escape jumps [19–22]. These escape jumps are present throughout development [23,24] and can generate speeds of up to 800 mm s^{-1} and accelerations of up to 200 m s^{-2} [20]. The interaction of copepods and their natural predators has been investigated in a liquid medium [22,25,26]. However, aerial escapes have never been investigated for a planktonic organism, but may have significant ecological and evolutionary implications for the wide variety of species that live and feed within the surface layer of the ocean.

Reports of copepods breaking through the water surface occurred as early as the late nineteenth century [27]. The observer hypothesized that the leaps into the air and subsequent re-entry into the water functioned as a mechanism to assist with moulting, by jarring them loose from their old exoskeleton. A later report of aerial copepod jumps proposed an anti-predator mechanism [28], but the function of this behaviour remained hypothetical.

Using field video recordings and high-speed video in the laboratory, we demonstrate that aerial jumps provide an effective escape mechanism in response to visual fish predators. Kinematic analysis of this little-known behaviour reveals a significant energetic cost of breaking the water surface, yet this aerial escape behaviour still provides a net energy saving relative to an escape performed solely underwater. These findings provide insight into how this group of animals can be successful in a pelagic environment where they appear conspicuous and easily targeted by visual predators.

Received 23 January 2012
Accepted 28 February 2012

2. MATERIAL AND METHODS

(a) *Field recordings*

Field recordings were made using a hand-held video recorder at 30 frames s^{-1} (Sony Handycam CCD-TR3300) above the water surface. Recordings were edited in Adobe Premier Pro to maximize distinction between copepods and the surrounding water by adjusting both brightness and contrast. Two-dimensional escape kinematics in response to fish predators was obtained using ImageJ v. 1.43 software. Statistical analysis for both laboratory and field recordings was performed using SigmaPlot v. 11.0 (Systat Software Inc).

Field recordings of the copepod *Anomalocera ornata* interacting with juvenile mullet (*Mugil cephalus*) were performed for 15 min at the University of Texas Marine Science Institute marina, and escape responses from 89 individuals were obtained during analysis. The movement of the camera required to follow individual fish interacting with copepods made simple size and distance calibrations inappropriate. Instead, we captured and measured 22 of the juvenile *M. cephalus* that were in the location of the video recordings and the resulting standard length of 24.2 mm (s.d. 1.96) was used to scale the video frames during kinematic analysis. This method does not provide the finest spatial resolution, but allows a reasonable approximation of both distance and velocity. It should be noted that the calculated kinematic values represent minimum estimates of both velocity and distance, since recordings were based solely in an x–y plane normal to the camera lens, so any z component of motion was not accounted for. Therefore, velocity and distance are probably underestimated, but this effect is minimal for the laboratory studies since the narrow (4 cm width) aquarium limited movement in the z plane.

(b) *Laboratory recordings*

Copepods (*Labidocera aestiva*) were collected from inshore waters of the northern Gulf of Mexico (27°50′19″ N, 97°3′8″ W) using a 0.5 m diameter plankton net (150 µm mesh). Approximately 50 individuals were placed in a small, narrow rectangular acrylic aquarium (2 × 4 × 20 cm) filled to 50 per cent capacity with filtered seawater. A high-speed camera (Redlake MotionMeter model 1140-0003) equipped with a Nikon Nikkor 55 mm lens was used to capture the escape behaviour. Dark-field illumination was provided by infrared light emitting diodes (peak wavelength 890 nm). The copepod escape jumps were recorded at 250–500 frames s^{-1}. After 10 recordings, copepods were replaced with 50 new animals to limit the probability of recording the same animal multiple times.

Two camera positions were used during laboratory recordings. In position 1, the camera was aligned with the aquarium so that the surface of the water was near the bottom of the field of view in order to capture the entire aerial portion of the escape, and 60 escapes were recorded using this configuration. In position 2, the camera was oriented so that approximately one-third of the field of view was below the surface of the water and two-thirds was above the water surface. This allowed determination of the copepod's speed as it broke the water's surface, the contact angle to the surface and the trajectory through air. Twenty-four escapes were recorded with this configuration. The contact angle was determined at the instant contact was made at the water surface, while the entire animal remained underwater. Using image analysis software (ImageJ), we determined the angle using the water surface and the longitudinal central plane of the animal. Recordings were performed in a darkroom and escape responses from the copepods were elicited through a photic startle response by a rapid change in light intensity [29]. The subsequent escape responses resulted in many copepods breaking the water's surface and travelling variable distances through the air. Escapes in which more than 50 per cent of the aerial trajectory was out of the field of view were not used for analysis. In cases where only a smaller portion (less than 50%) of the escape travelled beyond the field of view, the maximal distance was extrapolated using Vogel's model for an object in free fall [30]. This was required for 19 of the 60 escapes used in our analysis.

(c) *Data analysis*

To compare the kinematic results obtained from both ImageJ v. 1.43 software and CellTrak v. 1.5 motion analysis software, data were log transformed and checked for normality using a Shapiro–Wilk test. A one-way analysis of variance (ANOVA) was performed for both total horizontal distance and maximum velocity.

We used the following equation to estimate the net kinetic energy loss (ΔK) incurred from a copepod breaking the water surface:

$$\Delta K = 0.5\, m_{\text{copepod}}(U_0^2 - U_1^2), \tag{2.1}$$

where m_{copepod} is the body mass of the copepod, U_0 is the copepod velocity at the moment just before the copepod starts to break the water surface and U_1 is the copepod velocity at the moment immediately after the copepod becomes completely airborne. $m_{\text{copepod}} = \rho_{\text{copepod}} \times V_{\text{copepod}}$, where ρ_{copepod} is the mass density of the copepod (approximately equal to the mass density of the seawater, ρ_{seawater}), and V_{copepod} is the copepod body volume. V_{copepod} is calculated as $4/3\pi\eta^2 a^3$, where a is half the prosome length and η the copepod aspect ratio, assuming the shape of a prolate spheroid with the long axis equal to the prosome length ($2a$) and the short axis equal to $\eta \times 2a$.

Here, we estimate three likely contributions to this energy loss:

(i) The loss owing to the water drag can be estimated as

$$\Delta K_1 = 0.25\, C_{\text{d}} \rho_{\text{seawater}}\, U_0^2\, S_{\text{e}}\, d_{\text{e}}, \tag{2.2}$$

where C_{d} is the drag coefficient of the equivalent sphere having the same volume as that of the copepod body, S_{e} is the cross-sectional area of the equivalent sphere and d_{e} is the diameter of the equivalent sphere. We estimate this energy loss during breaking the water surface (very short time scale) as the average between the moment the animal makes contact with the surface (fully underwater) and moment the animal fully breaks free of the surface (fully in air). Here, we assume that the drag acting on the copepod when it just starts to break the water surface is $0.5\, C_{\text{d}}\, \rho_{\text{seawater}}\, U_0^2\, S_{\text{e}}$, and the drag acting on the copepod when it just leaves the water surface to become completely airborne is $0.5\, C_{\text{d}}\, \rho_{\text{air}}\, U_1^2\, S_{\text{e}}$, where ρ_{air} is the mass density of air. Because $\rho_{\text{air}} \ll \rho_{\text{seawater}}$, the average drag for this short time interval is approximately $0.25\, C_{\text{d}}\, \rho_{\text{seawater}}\, U_0^2\, S_{\text{e}}$. The average drag multiplied by the distance travelled, d_{e}, leads to equation (2.2). C_{d} is calculated based on the Reynolds number, $\text{Re} = U_0\, d_{\text{e}} / \nu_{\text{seawater}}$, where ν_{seawater} is the kinematic viscosity of the seawater. Although we are not sure about the

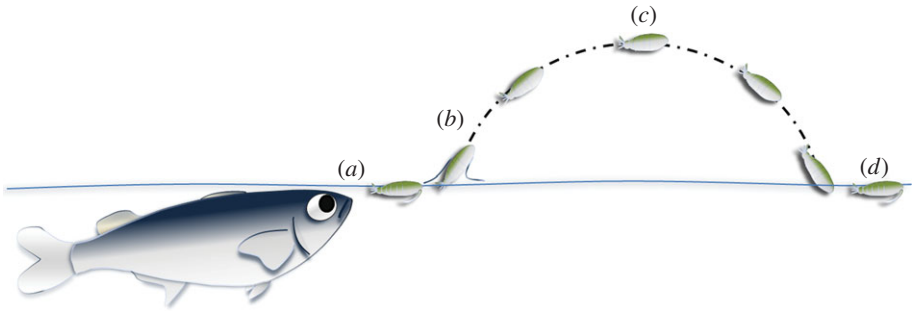

Figure 1. Representative diagram showing the response of the copepod *Anomalocera ornata* to the approach of a planktivorous fish predator (juvenile *Mugil cephalus*). The fish swims in a random cruising pattern just below the water surface until visually encountering a copepod. (*a*) Once located visually, the fish swims towards the copepod and attempts to ingest it. (*b*) The approach of the fish alerts the copepod to the presence of a potential predator and the copepod responds with an aerial leap. (*c*) The copepod travels many times its own body length and significantly further than a single escape underwater to exit the perceptive field of the predator. (*d*) Once the copepod re-enters the water it resumes swimming at the surface. Not drawn to scale.

applicability of the commonly used drag law, equation (2.2) should give upper bound estimation of the energy loss owing to the water drag.

(ii) The loss owing to the increase of the gravitational potential energy of the copepod body estimated as

$$\Delta K_2 = m_{\text{copepod}}\, g\, d_e\, \cos(\alpha), \tag{2.3}$$

where g is acceleration owing to gravity and α is the exit angle (electronic supplementary material, figure S1).

(iii) The loss owing to overcoming the surface tension:

$$\Delta K_3 = \sigma A_{\text{copepod}}\, \cos(\theta), \tag{2.4}$$

where σ ($= 0.075\ \text{N m}^{-1}$) is the surface tension for the seawater–air interface, A_{copepod} is the surface area of the copepod, and θ is the contact angle between the copepod body and the seawater surface. Here, we assume that the energy loss is due to the copepod surface condition changing from interfacing with seawater to interfacing with air, such that $\Delta K_3 = (\sigma_{\text{copepod-air}} - \sigma_{\text{copepod-seawater}})A_{\text{copepod}}$, where $\sigma_{\text{copepod-air}}$ and $\sigma_{\text{copepod-seawater}}$ are the surface energies associated with the copepod–air and copepod–seawater interfaces, respectively. Using Young's law for the contact angle (i.e. $\sigma_{\text{copepod-air}} = \sigma_{\text{copepod-seawater}} + \sigma\ \cos(\theta)$ [31]) we obtain equation (2.4).

3. RESULTS

Field video recordings captured the copepod *Anomalocera ornata* (prosome length 2.5–3.1 mm) in the presence of small plankton-feeding fish (juvenile *Mugil cephalus*) within inshore waters of the northern Gulf of Mexico. The escape behaviour was stimulated by the approach of the predatory fish, *M. cephalus* (figure 1), and consisted of an airborne leap covering a horizontal distance of 80 ± 0 mm ($n = 89$), with maximum distances of up to 170 mm observed (see electronic supplementary material for video of this behaviour). On average, the copepods travelled over 40 times their own body length and 3.4 times the body length of the fish predator (mean standard length 24.2 mm). The maximum aerial velocity achieved during these escapes was $890 \pm 200\ \text{mm s}^{-1}$ and average velocities over the entire escape were $660 \pm 150\ \text{mm s}^{-1}$ (figure 2*a*). Only one of the 89 observed escapes resulted in multiple attacks by the same fish.

A smaller pontellid copepod (prosome length 1.8–2.0 mm), *Labidocera aestiva*, was stimulated to perform escape jumps in the laboratory using a photic startle response, and the escapes were recorded with a high-speed video camera at 250–500 frames s^{-1} (see electronic supplementary material for video of this behaviour). This species swam approximately 0–40 mm below the water's surface until stimulated to escape. We found the maximum aerial velocity of the copepods after they broke the water's surface to be $630 \pm 150\ \text{mm s}^{-1}$. This was significantly lower ($p = <0.001$) than velocities produced by *A. ornata* and also resulted in significantly lower ($p = <0.001$) horizontal escape distances (figure 2*a*). *Labidocera aestiva* was able to attain heights over 60 mm above the water's surface and up to 76 mm in distance from the exit point in the water. However, the mean horizontal distance travelled during escapes through air was 16.0 ± 14.1 mm. It is interesting to note that in most cases, rotation was imparted on the animal as it broke the surface (see electronic supplementary material, video). In some cases, the rotation was estimated in excess of 45 000 degrees s^{-1} (7500 r.p.m.). The underwater portion of the escapes for *L. aestiva* yielded maximum velocities of $1036 \pm 121\ \text{mm s}^{-1}$, which is significantly greater ($p = <0.001$) than maximum velocities observed after breaking the surface.

The results of a correlation analysis between horizontal escape distance and maximum aerial velocity for *A. ornata* exhibited a moderate relationship ($R^2 = 0.36$; figure 2*b*). The same analysis performed for *L. aestiva* exhibited virtually no correlation between horizontal escape distance and maximum aerial velocity ($R^2 = 0.04$; figure 2*c*). Notably, swimming pattern and orientation of the two species relative to the water surface before escape are also different (figure 3). *Labidocera aestiva* was observed to swim freely below the water surface using an intermittent (cruising–sinking) swimming pattern. During the cruising phase, the copepod was oriented randomly to the water surface, but during sinking *L. aestiva* was consistently observed to orient with its anterior end towards the water surface. *Anomalocera ornata* exhibited a cruising swimming pattern, and was consistently oriented with its ventral side facing

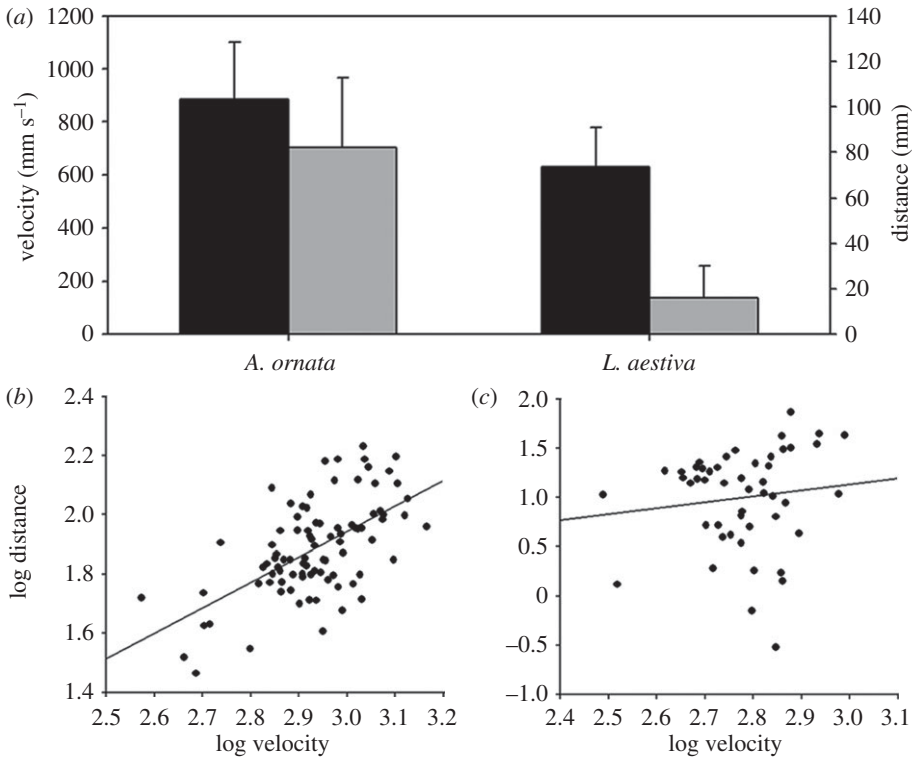

Figure 2. (*a*) Relationship between horizontal distance and maximum aerial velocity for two species of copepods during airborne escapes. *Anomalocera ornata* exhibits a significantly greater horizontal distance ($p = <0.001$, one-way ANOVA) and aerial velocity ($p = <0.001$, one-way ANOVA) than *Labidocera aestiva*. The larger copepod, *A. ornata*, is able to travel proportionally further per unit energy. Maximum aerial velocity was obtained at the moment the animal fully exited the water surface. Error bars represent s.d. Black bars, velocity; grey bars, distance. Regression plot for (*b*) *A. ornata* ($R^2 = 0.36$) and (*c*) *L. aestiva* ($R^2 = 0.04$), where *A. ornata* shows a stronger correlation of velocity with distance.

downwards (away from the surface) and the dorsal side of the animal at the water surface.

When high-speed recordings during the aerial portion of an escape jump of *L. aestiva* are compared with a model of biological projectiles [29], the copepod acts as a ballistic object in free fall (figure 4*a*). Using data from both 500 and 250 frame s^{-1} observations, we estimate that 58 to 88 per cent of the kinetic energy at the moment when the copepod starts to break the water surface will be lost for breaking the water surface (figure 4*b*). Among the total loss (fitted to the data), 61 to 67 per cent is due to overcome the water drag force (i.e. ΔK_1), the contribution from increases of gravitational potential energy (ΔK_2) is negligible, and the loss owing to overcoming the surface tension (ΔK_3) is 33 to 39 per cent. When a similar calculation is made for adult flying fish that are orders of magnitude larger than pontellid copepods, yet produce a functionally analogous behaviour, the cost of breaking the surface is less than 0.07 per cent of the kinetic energy possessed at the moment when the fish starts to break the water surface.

4. DISCUSSION

Large-scale movement of copepods that reside in the neustonic surface layer of the ocean is often subject to surface currents. They have been observed to accumulate at oceanic frontal boundaries [32], where small predatory fish are also more abundant [33]. Thus, successful predator evasion is essential to the copepod's survival. However, being confined at the surface limits escape ability, and predators have been observed using the water surface to aid in prey capture [34]. The ability of some pontellid copepods to break the water surface provides advantages over escapes that occur solely underwater. First, exiting the perceptive field of a predator and re-entering at a random location reduces the chance of continued pursuit, and the 80 ± 30 mm horizontal escape distance observed for *A. ornata* is well beyond the perceptive distance determined for fish of similar length to *C. mugil* [35]. Second, for a copepod to achieve a similar escape distance solely underwater, it would have to expend approximately 20 times more mechanical energy; therefore a significant energetic saving exists by jumping into air.

The underwater velocity is higher than maximum velocities reported for other similarly sized copepods [20], which facilitate these small organisms breaking the water surface. However, the mode in which the two species of copepods exit the water is different (figure 3). *Anomalocera ornata* consistently swims with its dorsal side at the water surface, while the anterior end of *L. aestiva* was generally directed towards the surface but was observed to swim at many orientations just below the surface. This may explain why *L. aestiva* exhibits a lower correlation between maximum aerial velocity and horizontal distance than *A. ornata* (figure 2*b*,*c*).

Considering a single-stroke escape jump that occurs completely underwater, the copepod achieves its peak velocity approximately at the end of the power stroke of the swimming legs. During the power stroke, the copepod

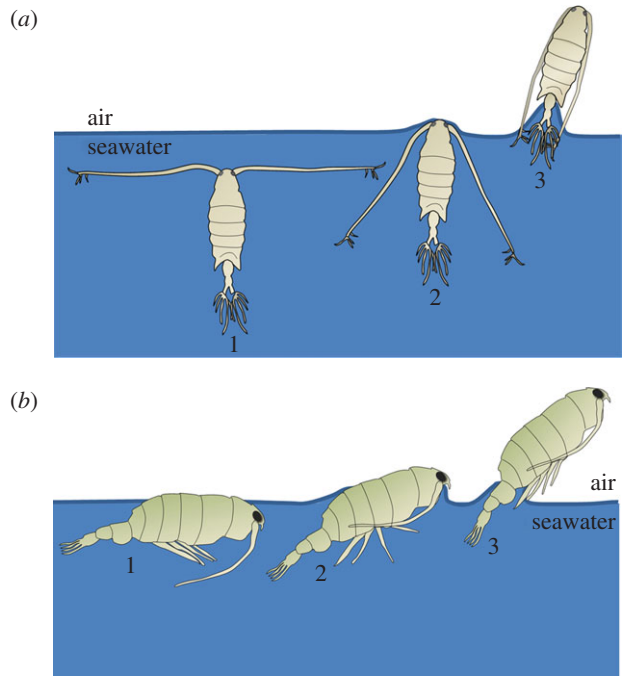

Figure 3. Two observed techniques used by neustonic copepods to break through surface tension of seawater during aerial escape responses. (*a*) *Labidocera aestiva* swims below the surface and is often oriented with the anterior portion of its body towards the water surface (1). (*b*) *Anamolcera ornata* swims at the air–water interface with its dorsal side facing the surface and ventral side facing downwards (1). (*a*,*b*) After being stimulated to perform an escape, swimming appendages (pereiopods) of both species beat sequentially as antennae fold against the body as the animal is propelled forward (2). As the animals accelerate, the increase in kinetic energy allows the body to overcome surface tension forces and travel through the air (3).

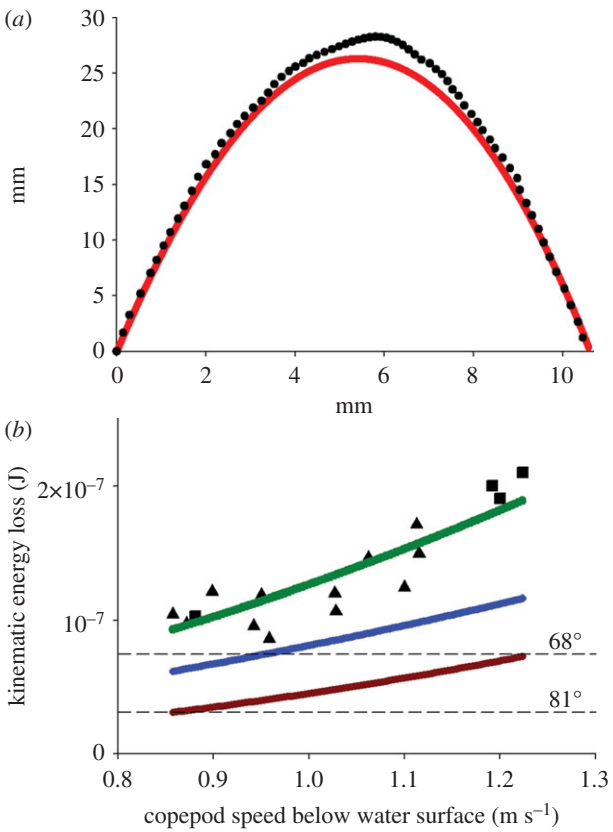

Figure 4. (*a*) Observed copepod trajectory during airborne versus a ballistic/free-fall model prediction. Red line, free-fall model; black circles, actual trajectory. (*b*) Kinetic energy loss as a function of the copepod (maximum) speed below water surface. The squares label the data obtained via 500 frame s^{-1} video recording, and the triangles label the data obtained via 250 frame s^{-1} video recording. The solid green line is a fit to the data ($\Delta K = 1.26 \times 10^{-7}\ U_0^2$, where U_0 is the copepod speed below water surface). The solid blue line is the contribution to the kinetic energy loss owing to water drag. The solid red line is the difference between the green line and the blue line. The two dashed horizontal lines represent the work needed to overcome the surface tension in order for the copepod to be airborne for two assumed receding contact angles between the copepod and the sea–water interface (calculated from equation (2.4) for a constant $\sigma = 0.075$ N m^{-1}). Note that the red line is bounded between these two dashed horizontal lines. Copepod prosome length = 1.8 mm, and aspect ratio = 0.32.

travels a distance nL, where L is the prosome length and n approximately 1–2 [21]. Upon completion of the power stroke, the copepod rapidly decelerates owing to drag forces, but maintains enough inertia to move forward another distance of approximately nL until coming to rest. The present observations show that copepods, via a one-kick jump, can break the surface of the water (see electronic supplementary material, video) and peak velocity (U_0) is obtained just before breaking the surface. At the moment when the animal becomes completely airborne, it travels at a velocity (U_1) that is significantly smaller than U_0. In other words, there is a net kinetic energy loss (figure 4*b*). The net kinetic energy loss (ΔK) incurred during the copepod *Labidocera aestiva* breaking the water surface is 58 to 88 per cent.

This energy loss, however, is compensated for by increased escape distance. After becoming airborne, the copepod can travel significantly farther than nL (i.e. the distance it otherwise travels underwater) because it now experiences the air mass density, which is approximately 850 times smaller than the mass density of seawater. Therefore, the copepod will experience less drag, resulting in increased distance. There is no propulsive force exerted by the copepod after it becomes airborne, and the copepod undergoes ballistic motion because of gravity (and the air drag force; figure 4*a*).

Our field observations show that copepods can effectively use aerial escapes as an anti-predator mechanism. By leaving the perceptive environment of the visual fish predators and re-entering the water up to 170 mm (approx. 60 body lengths) away from the attack site, a copepod can use this effective strategy, which appears analogous to that of some larger organisms (e.g. flying fish). An important difference, however, is that all species known to perform similar types of behaviour are orders of magnitude larger than copepods. This means that copepods must contend with the reduced inertial forces (lower Reynolds number) and a greater proportion of the total energy dedicated to break the surface tension of water.

Consider the case of a flying fish. We calculate that flying fish lose less than 0.07 per cent of their overall kinetic energy in breaking the surface tension, compared with 33 to 39 per cent in the case of the copepod, despite a greater magnitude of energy loss (owing to larger

surface area) than copepods. This is due to the fact that flying fish possess orders of magnitude more kinetic energy upon contact with the water surface because of much greater mass, and underwater speeds of approximately $10\ m\ s^{-1}$ [36] compared with approximately $1\ m\ s^{-1}$ in copepods. However, it should be noted that although aerial escapes in larger, heavier aquatic animals lose almost no kinetic energy from surface tension effects, horizontal distances in terms of body length (for animals exhibiting ballistic aerial motion) are much shorter [37]. Thus, what appears to be a disadvantage of small mass (e.g. losing significant proportion of kinetic energy) can translate into an advantage: once the water surface is broken, the copepod travels disproportionally farther than larger animals (with ballistic flight paths). The major reason for this is that the copepod has the ability to generate and maintain a disproportionally large air-entry velocity (relative to body length) compared with larger animals. A secondary reason might be that the flying copepod experiences smaller air-drag-induced deceleration than larger animals. Therefore, ballistic aerial escape paths can be effective in pelagic ecosystems when the animal (and predator) is small, but are unlikely to carry a larger animal out of the perceptive range of their predator. Instead, specialized structures and behaviour such as those observed in flying fish are required to extend horizontal distance above water.

Because escapes are energetically costly [38–40], a copepod's fitness can be reduced even without being captured by a predator. It therefore benefits the copepod to balance predation risk and energy cost by avoiding unnecessary escapes. To avoid pursuit or multiple attacks from a predator, copepods must travel to a distance outside of the perceptive range of the predator. During an escape, a copepod travels approximately one to two times its prosome length per stroke (calculated from Waggett & Buskey [21]). For the pontellid copepods, this would result in a distance of 2–6 mm per stroke. However, even small fish can perceive prey at least 10 mm away [35,41]; thus, multiple escape jumps are required for a copepod to exit the predator's perceptive field. Therefore, if an escape occurs in air rather than water, reduced drag forces can extend escape distance. This can transport a copepod further from a predator with a single escape jump than with multiple jumps in an aqueous environment, resulting in net energy savings. They also return to the water in an unpredictable location, making pursuit from the predators unlikely.

Finally, the pontellid copepods may have special adaptations to make it easier for them to jump out of the water. One possible adaptation is that the body surface of those copepod species that do perform such air-entering jumps is less wettable than other copepods or crustaceans in general, and thus their surface properties may be essential for their unusual capability of breaking the water surface. Our kinetic energy budget calculation suggests that if the surface tension is not altered during the breaking of the surface (i.e. a constant $\sigma = 0.075\ N\ m^{-1}$), in order to maintain a useful level of kinetic energy after breaking the surface the copepod body surface has to be hydrophobic, i.e. much larger contact angle in the 68–81° range (figure 4*b*; calculated according to equation (2.4)). Another suspected adaptation may be that the copepods inject chemicals during breaking of the surface to reduce the surface tension by three to six times, and therefore a useful level of air-entry kinetic energy can still be maintained even when the contact angle remains similar to published measurements for other crustaceans in the range of below 20° [42]. Further investigation is required to find out if these adaptations indeed exist. Nevertheless, unusual morphological structures are known to exist on the dorsal side of pontellid copepods [43], which might contribute to making the copepod body surface less wettable. However, these morphological structures make up only a small part of the animal's total surface. Alternatively, pores specialized for secretion onto the body surface exist in pontellids [44], and similar pores with currently unknown function may also be involved in secreting substances to alter surface properties or surface tension of water immediately surrounding the animal. Regardless of the mechanism, escaping through air appears to be an effective strategy to not only avoid and survive attacks from predators by temporarily exiting the liquid environment and exiting the predator's perceptive field, but also to conserve energy during escapes, providing a competitive advantage for pontellid copepods in the neustonic environment.

This work was supported by grants from the National Science Foundation, USA to E.J.B. (NSF OCE-0452159) and to H.J. (NSF OCE-1129496). C. Brown assisted B.J.G. with collection and E. Hing-Fay maintained copepods for J.R.S.

REFERENCES

1 Humes, A. G. 1994 How many copepods? *Hydrobiologia* **292/293**, 1–7. (doi:10.1007/BF00229916)
2 Turner, J. T. 2004 The importance of small planktonic copepods and their roles in pelagic marine food webs. *Zool. Stud.* **43**, 255–266.
3 Govoni, J. J. & Chester, A. J. 1990 Diet composition of larval *Leiostomus xanthurus* in and about the Mississippi River plume. *J. Plankton Res.* **12**, 819–830. (doi:10.1093/plankt/12.4.819)
4 Anderson, J. T. 1995 Feeding ecology and condition of larval and pelagic juvenile redfish *Sebastes* spp. *Mar. Ecol. Prog. Ser.* **104**, 211–226. (doi:10.3354/meps104211)
5 Hillgruber, N., Haldorson, L. J. & Paul, A. J. 1995 Feeding selectivity of larval walleye pollock *Theragra chalcogramma* in the oceanic domain of the Bering Sea. *Mar. Ecol. Prog. Ser.* **120**, 1–10. (doi:10.3354/meps120001)
6 Conway, D., Coombs, S. H. & Smith, C. 1998 Feeding of anchovy *Engraulis encrasicolus* larvae in the northwestern Adriatic Sea in response to changing hydrobiological conditions. *Mar. Ecol. Prog. Ser.* **175**, 35–49. (doi:10.3354/meps175035)
7 Costello, J. H. & Colin, S. P. 1994 Morphology, fluid motion and predation by the scyphomedusa *Aurelia aurita*. *Mar. Biol.* **121**, 327–334. (doi:10.1007/BF00346741)
8 Oresland, V. 1995 Winter population structure and feeding of the chaetognath *Eukrohnia hamate* and the copepod *Euchaeta antarctica* in Gerlache Strait, Antarctic Peninsula. *Mar. Ecol. Prog. Ser.* **119**, 77–86. (doi:10.3354/meps119077)
9 Sieburth, J. M. *et al.* 1976 Dissolved organic matter and heterotrophic microneuston in the surface microlayers of the North Atlantic. *Science* **194**, 1415–1418. (doi:10.1126/science.194.4272.1415)
10 Brodeur, R. D. 1989 Neustonic feeding by juvenile salmonids in coastal waters of the Northeast Pacific. *Can. J. Zool.* **67**, 1995–2007. (doi:10.1139/z89-284)

11 Tester, P. A., Cohen, J. H. & Cervetto, G. 2004 Reverse vertical migration and hydrographic distribution of *Anomalocera ornata* (Copepoda: Pontellidae) in the US south Atlantic bight. *Mar. Ecol. Prog. Ser.* **268**, 195–203. (doi:10.3354/meps268195)
12 Hansson, L. A. 2000 Induced pigmentation in zooplankton: a trade-off between threats from predation and ultraviolet radiation. *Proc. R. Soc. Lond. B* **267**, 2327–2332. (doi:10.1098/rspb.2000.1287)
13 Herring, P. J. 1965 Blue pigment of a surface-living oceanic copepod. *Nature* **205**, 103–104. (doi:10.1038/205103a0)
14 Byron, E. R. 1982 The adaptive significance of calanoid copepod pigmentation: a comparative and experimental analysis. *Ecology* **63**, 1871–1886. (doi:10.2307/1940127)
15 Hansson, L. A., Hylander, S. & Sommaruga, R. 2007 Escape from UV threats in zooplankton: a cocktail of behavior and protective pigmentation. *Ecology* **88**, 1932–1939. (doi:10.1890/06-2038.1)
16 Mauchline, J. 1998 *The biology of calanoid copepods*. Advances in Marine Biology, vol. 33. San Diego, CA: Academic Press.
17 Brooks, J. L. & Dodson, D. I. 1965 Predation, body size, and composition of the plankton. *Science* **150**, 28–35. (doi:10.1126/science.150.3692.28)
18 Morgan, S. G. & Christy, J. H. 1996 Survival of marine larvae under the countervailing selective pressures of photodamage and predation. *Limnol. Oceanogr.* **41**, 498–504. (doi:10.4319/lo.1996.41.3.0498)
19 Buskey, E. J., Lenz, P. H. & Hartline, D. K. 2002 Escape behavior of copepods in response to hydrodynamic disturbances: high speed video analysis. *Mar. Ecol. Prog. Ser.* **235**, 135–146. (doi:10.3354/meps235135)
20 Lenz, P. H., Hower, A. E. & Hartline, D. K. 2004 Force production during pereiopod power strokes in *Calanus finmarchicus*. *J. Mar. Syst.* **49**, 133–144. (doi:10.1016/j.jmarsys.2003.05.006)
21 Waggett, R. J. & Buskey, E. J. 2007 Calanoid copepod escape behavior in response to a visual predator. *Mar. Biol.* **150**, 599–607. (doi:10.1007/s00227-006-0384-3)
22 Viitasalo, M., Kiørboe, T., Flinkman, J., Pedersen, L. W. & Visser, A. W. 1998 Predation vulnerability of planktonic copepods: consequences of predator foraging strategies and prey sensory abilities. *Mar. Ecol. Prog. Ser.* **175**, 129–142. (doi:10.3354/meps175129)
23 Buskey, E. J. 1994 Factors affecting feeding selectivity of visual predators on the copepod *Acartia tonsa:* locomotion, visibility and escape responses. *Hydrobiology* **292/293**, 447–453. (doi:10.1007/BF00229971)
24 Titelman, J. & Kiørboe, T. 2003 Predator avoidance by nauplii. *Mar. Ecol. Prog. Ser.* **247**, 137–149. (doi:10.3354/meps247137)
25 Waggett, R. J. & Buskey, E. J. 2007 Copepod escape behavior in non-turbulent and turbulent hydrodynamic regimes. *Mar. Ecol. Prog. Ser.* **334**, 193–198. (doi:10.3354/meps334193)
26 Ohman, M. D. 1986 Predator-limited population growth of the copepod *Pseudocalanus* sp. *J. Plankton Res.* **8**, 673–713. (doi:10.1093/plankt/8.4.673)
27 Astroumoff, A. 1894 A flying copepod. *J. R. Microsc. Soc.* **14**, 618.
28 Zaitsev, Y. P. 1971 *Marine neustonology*. Springfield, VA: National Marine Fisheries Service, NOAA and National Science Foundation, National Technical Information Service.
29 Buskey, E. J. & Hartline, D. K. 2003 High speed video analysis of the escape responses of the copepod *Acartia tonsa* to shadows. *Bio. Bull.* **204**, 28–37. (doi:10.2307/1543493)
30 Vogel, S. 2005 Living in a physical world II. The bioballistics of small projectiles. J. Biosci. **30**, 167–175. (doi:10.1007/BF02703696)
31 de Gennes, P. G., Brochard-Wyart, F. & Quéré, D. 2003 *Capillarity and wetting phenomena: drops, bubbles, pearls, waves*. New York, NY: Springer.
32 Turner, J. T., Tester, P. A. & Hettler, W. F. 1985 Zooplankton feeding ecology. *Mar. Biol.* **90**, 1–8. (doi:10.1007/BF00428208)
33 Govoni, J. J. & Grimes, C. B. 1992 The surface accumulation of larval fishes by hydrodynamic convergence within the Mississippi River plume front. *Cont. Shelf Res.* **12**, 1265–1276. (doi:10.1016/0278-4343(92)90063-P)
34 Bonfil, R. 2009 The biology and ecology of the silky shark, *Carcharhinus Falciformis*. In *Sharks of the open ocean: biology, fisheries and conservation* (eds M. D. Camhi, E. K. Pikitch & E. A. Babcock), pp. 114–127. Oxford, UK: Blackwell Publishing Ltd.
35 Miller, T. J., Crowder, L. B. & Rice, J. A. 1993 Ontogenetic changes in behavioural and histological measures of visual acuity in three species of fish. *Environ. Biol. Fishes* **37**, 1–8. (doi:10.1007/BF00000707)
36 Davenport, J. 1994 How and why do flying fish fly? *Rev. Fish Biol. Fisheries.* **4**, 184–214. (doi:10.1007/BF00044128)
37 Saidel, W. M., Strain, G. F. & Fornari, S. K. 2004 Characterization of the aerial escape response of the African Butterfly Fish, *Pantodon buchholzi* Peters. *Environ. Biol. Fishes.* **71**, 63–72. (doi:10.1023/B:EBFI.0000043153.38418.cd)
38 Strickler, J. R. 1975 Swimming of planktonic *Cyclops* species (Copepoda, Crustacea): pattern, movements and their control. In *Swimming and flying in nature* (eds T.Y.T. Wu, C. J. Brokaw & C. Brennen) pp. 599–613. Princeton, NJ: Plenum Press.
39 Alcaraz, M. & Strickler, J. R. 1988 Locomotion in copepods: patterns of movement and energetic of *Cyclops*. *Hydrobiology* **167/168**, 409–414. (doi:10.1007/BF00026333)
40 Marrase, C., Costello, J. H., Granata, T. & Strickler, J. R. 1990 Grazing in a turbulent environment: energy dissipation, encounter rates, and efficacy of feeding currents in *Centropages hamatus*. *Proc. Natl Acad. Sci. USA* **87**, 1653–1657. (doi:10.1073/pnas.87.5.1653)
41 Hunt von Herbing, I. & Gallager, S. M. 2000 Foraging behavior in early Atlantic cod larvae (*Gadus morhua*) feeding on a protozoan (*Balanion* sp.) and a copepod nauplius (*Pseudodiaptomus* sp.). *Mar. Biol.* **136**, 591–602. (doi:10.1007/s002270050719)
42 Becker, K., Hormchong, T. & Wahl, M. 2000 Relevance of crustacean carapace wettability for fouling. *Hydrobiologia* **426**, 193–201. (doi:10.1023/A:1003918512565)
43 Ianora, A., Miralto, A. & Vanucci, S. 1992 The surface attachment structure: a unique type of integumental formation in neustonic copepods. *Mar. Biol.* **113**, 401–407. (doi:10.1007/BF00349165)
44 Blades, P. I. & Youngbluth, M. J. 1979 Mating behavior of *Labidocera aestiva* (Copepoda: Calanoida). *Mar. Biol.* **51**, 339–355. (doi:10.1007/BF00389212)

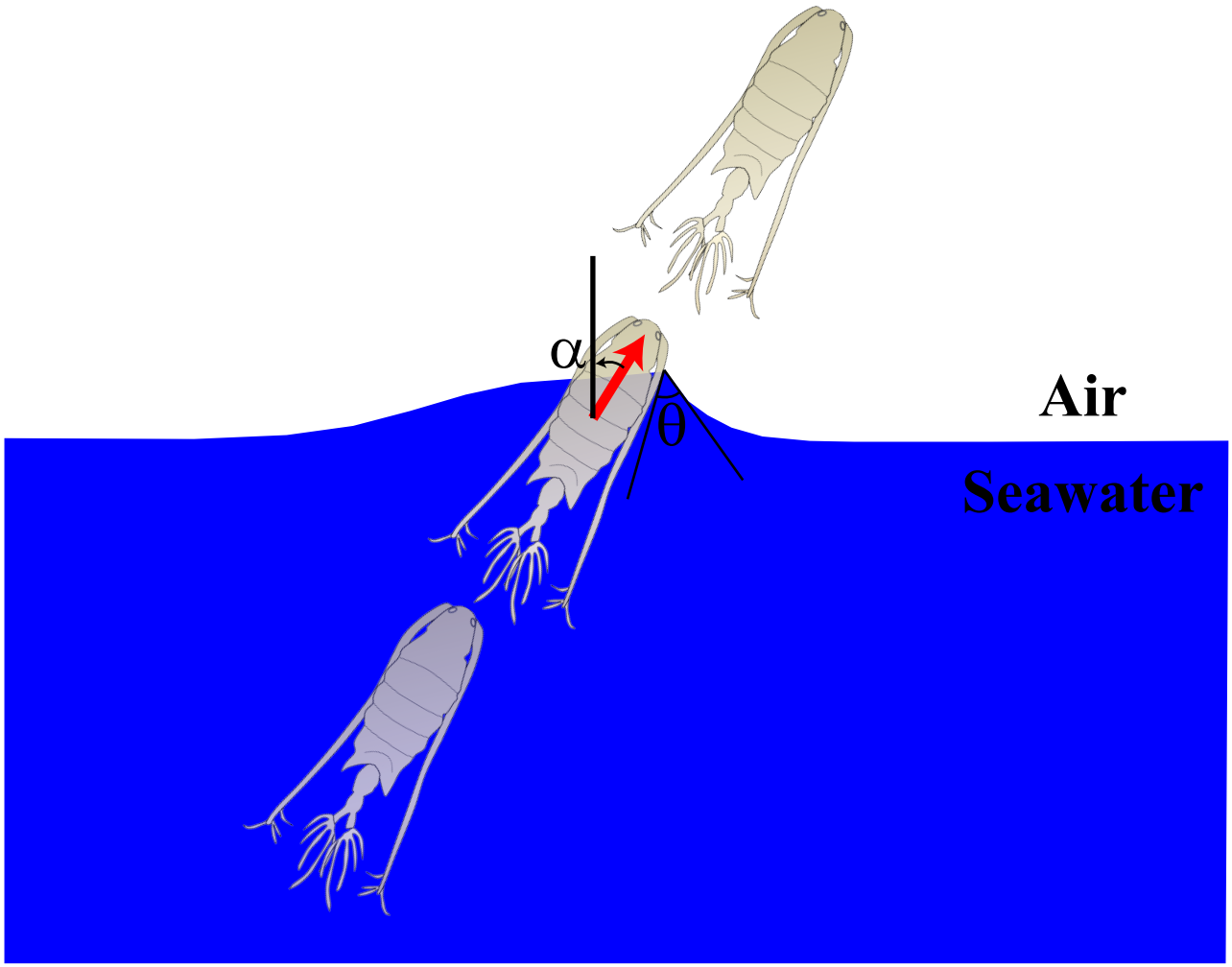

Figure S1. A highly hypothetical schematic of a copepod breaking the air-seawater interface to become completely airborne. The angle α is defined as the exit angle, and the angle θ is the contact angle between the copepod body and the seawater surface.

ENERGY LOSS OWING TO OVERCOMING SURFACE TENSION FOR FLYING FISH

Houshuo Jiang
Woods Hole Oceanographic Institution
Woods Hole, MA 02543

For "Gemmell, B.J., Jiang, H., Strickler, J.R., & Buskey, E.J. (2012) Plankton reach new heights in effort to avoid predators. *Proc. R. Soc. B*, doi: 10.1098/rspb.2012.0163."

L: Fish body length [= 0.23 m, averaged using data in Table 1 of Davenport (1994)];

W: Fish body width [= $\eta \times L$, where the aspect ratio $\eta \sim 0.2$ based on Fig. 1 of Davenport (1994)];

U: Velocity at which the flying fish approaches the sea surface (about 10 m s^{-1} in such large animals; some 20-30 body lengths s^{-1}) with its lateral fins furled against the body [Page 195 in Davenport (1994)]. Here, we use $U = 20 \times L$ (in m s^{-1}) for a conservative estimation;

ρ: Mass density of the fish (~ 1090 kg m^{-3});

σ: Surface tension for the seawater-air interface (= 0.075 N m^{-1});

θ: Contact angle between the fish body and the seawater surface, which is assumed to be equal to zero degree for a conservative estimation;

A_{fish}: Surface area of the fish, which is approximately calculated by assuming the fish body as a prolate spheroid:

$$A_{\text{fish}} = \frac{\pi}{2}\eta L^2\left(\eta + \frac{\beta}{\sin(\beta)}\right), \text{ where } \beta = \arccos(\eta) \quad (1)$$

K: Total kinetic energy:

$$K = \frac{\pi}{12}\rho\eta^2 L^3 U^2 \quad (2)$$

The energy loss owing to overcoming the surface tension:

$$\Delta K_s = \sigma A_{\text{fish}} \cos(\theta) \quad (3)$$

Substituting the numbers, we obtain: A_{fish} = 0.0266 m^2, K = 2.94 Joule, and ΔK_s = 0.00199 Joule. Therefore, $\Delta K_s/K$ = 0.068 %.

Reference:

Davenport, J. (1994) How and why do flying fish fly? *Reviews in Fish Biology and Fisheries* 4:184-214.